

SETTING COMPONENT PROPERTIES IN INCREMENTAL FORMING

F. Maaß¹, M. Dobecki², M. Hahn¹, W. Reimers², A. E. Tekkaya¹

¹Institute of Forming Technology and Lightweight Components,
TU Dortmund University, Baroper Str. 303, 44227 Dortmund, Germany

²Institute for Materials Science and Technology - Metallic Materials,
TU Berlin University, Ernst-Reuter-Platz 1, 10587 Berlin, Germany

Keywords: Single Point Incremental Forming, Residual Stress State, Fatigue Strength

Abstract: The mechanical properties of formed components are significantly influenced by the prevailing residual stress state. Single point incremental sheet metal forming is a flexible manufacturing process for complex shaped parts that enables to adjust the residual stress state by a variation of the process parameters. In this paper, truncated cone geometries with increasing relative tool step-down increments are cyclically loaded to analyze the influence of the process parameters on the fatigue strength of the formed components. The fatigue strength decreases due to resulting tensile residual stresses on the tool-side of the cone with decreasing relative tool step-down increments. The maximum reduction of the fatigue strength caused by residual stresses is 42% in the investigated range of the relative tool step-down increments. The tensile residual stress amplitudes on the tool-side increase with an increasing number of step-down increments for the same final geometry.

1 Introduction

Individual product design to meet customized product requirements leads to a high product variety that demands flexible manufacturing processes [1]. For these applications, besides conventional forming processes, incremental sheet forming (ISF) processes can be used where a metal sheet is formed by the progression of localized deformation [2]. Incremental sheet forming (ISF) processes are characterized by a short development time and low tool costs [3] especially for small batch sizes. The single point incremental forming process (SPIF) is performed on a conventional CNC milling machine [4] where a geometry independent forming tool forms hollow parts without the need of dedicated dies. The forming tool with a hemispherical tool tip is moved along a preset toolpath to form the desired part shape while the sheet is clamped at the edges (see Figure 1a). Due to its incremental character, process parameters can be adjusted locally during the whole process to influence the mechanical properties of the formed component. It is well known that residual stresses affect mechanical component properties, in particular the fatigue strength of cyclically loaded components. Residual stresses in metal components can be thermally induced or by inhomogeneous plastic deformation during forming processes.

In recent literature it is shown how the residual stress state is influenced by adjusting the process parameters of the single point incremental forming process tool radius R_{tool} , step-down increment Δz , tool feed rate v_f , and rotational speed of the tool ω (see Figure 1b). The residual stress state of formed parts are analyzed based on a phenomenological evaluation of the influence of the process parameters [5]. The residual stress state of the sidewall of a truncated pyramid measured by the hole-drilling method shows a shift in the residual stress profile to the tensile range with increasing step-down increment Δz . An increase in the rotational speed of the tool ω lead to a decrease in the

near-surface residual stresses and an increase in the residual stress amplitudes in deeper material layers.

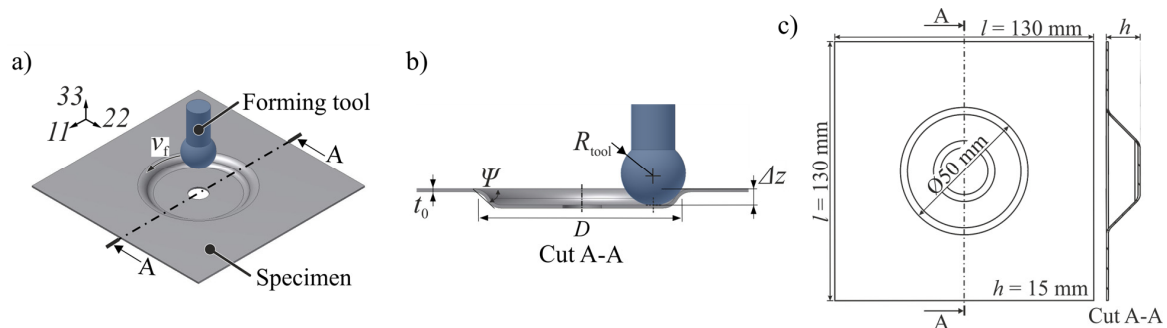


Figure 1. (a) Single point incremental forming process components and (b) process parameters (c) truncated cone geometry.

Maaß et al. [6] already showed numerically and based on metallurgical investigations the role of the relevant forming mechanisms shearing, bending and membrane stretching on the residual stresses of linear grooves.

To improve the product properties of a formed component, it is an important aspect how the SPIF process parameters influence the fatigue strength of a component due to the resulting residual stress state. This aspect has not been investigated yet. The knowledge of the fatigue strength is important especially for the component design regarding lightweight requirements. This paper deals with the influence of SPIF-induced residual stresses and how the process parameters affect the fatigue strength of the component. The results are based on numerical and experimental investigations on truncated cone geometries (see Figure 1c). The residual stresses are evaluated by x-ray diffraction (XRD) and the fatigue strength is evaluated by cyclic loading tests.

2 Experimental Procedure

The experimental design is based on a truncated cone geometry to compare the influence of the process parameters vertical step-down increment Δz and tool radius R_{tool} . Geometrical identically truncated cone geometries with three different relative step-down increments are manufactured. The residual stress state of the formed components is evaluated from a numerical process model and compared to XRD measurements. Afterwards, the specimens are cyclically loaded. For the evaluation of the residual stress influence on the fatigue strength, the results are compared with specimens that are stress-relieved by a heat treatment.

2.1 Manufacturing Process

The truncated cone geometries are manufactured by a five-axis CNC-milling machine DMG MORI DMU 50. The geometry is formed in a squared aluminum alloy 5083 sheet with an initial sheet thickness $t_0 = 1$ mm and an edge length $l = 130$ mm (see Figure 1c). A unidirectional toolpath strategy is used to form the truncated cone geometries to a final depth of $h = 15$ mm. The rotating forming tool is moved with a feed rate $v_f = 300$ mm/min. As a lubricant, the sheet metal surface is coated with a deep-drawing oil (Castrol Iloform PN 226) before starting the forming process. A variation of the relative step-down increment $\Delta z/R_{\text{tool}}$ is achieved by adjusting the step-down increment to $\Delta z_{0.25} = 1.25$ mm, $\Delta z_{0.5} = 2.5$ mm, and $\Delta z_{0.75} = 3.75$ mm. The tool radius $R_{\text{tool}} = 5$ mm is kept constant.

2.2 Numerical Model and Material Characterization

According to the experimental setup, the process is modelled numerically using the software ABAQUS. The numerical material model includes combined isotropic-kinematic hardening. For the forming process, the explicit solver is used. In a subsequent implicit simulation, the unclamping process is modelled to evaluate the residual stress state of the formed component. The sheet is modelled with solid elements with a mesh size of 1 mm in sheet plane direction and five elements in thickness direction (see Figure 3a). The forming tool is assumed rigid. The material parameters for the used aluminium alloy 5083 with an initial yield strength $\sigma_{y0} = 168$ MPa is based on material characterization using in-plane torsion tests and uniaxial tensile tests. The determined stress-strain curves of the base material are shown in Figure 3b. Further details on the numerical experiment can be found in Maaß et al. [7] where a different part geometry is formed.

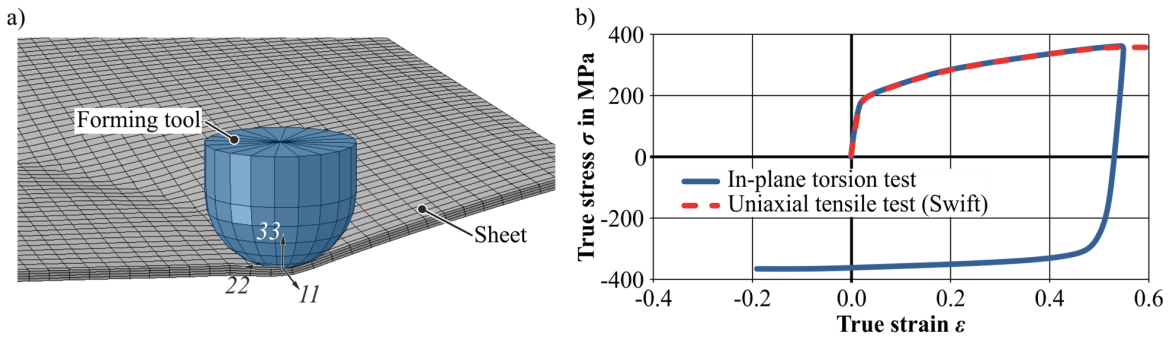


Figure 3. (a) Numerical process model and (b) stress-strain curve of the AA5083 base material.

2.3 Residual Stress Measurement and Evaluation

The residual stresses are evaluated in the middle of the curved surface opposite to the tool marks of the increment line. Residual stresses are evaluated in radial σ_{22} -direction on the tool-side and the tool-averted side (Figure 4a). XRD is used to experimentally analyze the residual near-to-surface stress state. The strain analysis is based on the determination of the interplanar spacing $d(hkl)$ (hkl -MILLER indices) according to BRAGG's law:

$$n\lambda = 2d(hkl)\sin\theta \quad (1)$$

where n describes the diffraction order of the interference (hkl), λ the wavelength, and θ their BRAGG angle. Corresponding to the tensorial character of strains and stresses, the interplanar lattice spacings are measured for different sample orientations. The stresses are calculated applying the $\sin^2\Psi$ method [8]. The measurements are performed on the aluminium-reflection 311. Using Co-K α radiation with a penetration depth of $\tau = 8$ μm , the reflection profile is measured in the 2θ angular range of 91.7° - 95.7° with a step size of $\Delta 2\theta = 0.05$ and a counting time of 15 s per step. A round collimator with a diameter of 1.5 mm is used. The diffracted beam is collimated with a 0.4 $^\circ$ -Soller and a LiF monochromator. The reflection profiles are acquired for 9 Ψ -tilts ($\pm 63.435^\circ$, $\pm 50.787^\circ$, $\pm 39.232^\circ$, $\pm 26.565^\circ$ and 0°) (see Figure 4a). For the evaluation of the residual stresses the diffraction elastic constants (DEK) $s_2 = 19.536 \cdot 10^{-6}$ MPa and $s_1 = -5.093 \cdot 10^{-6}$ MPa are employed. The measuring point is kept constant for all specimens.

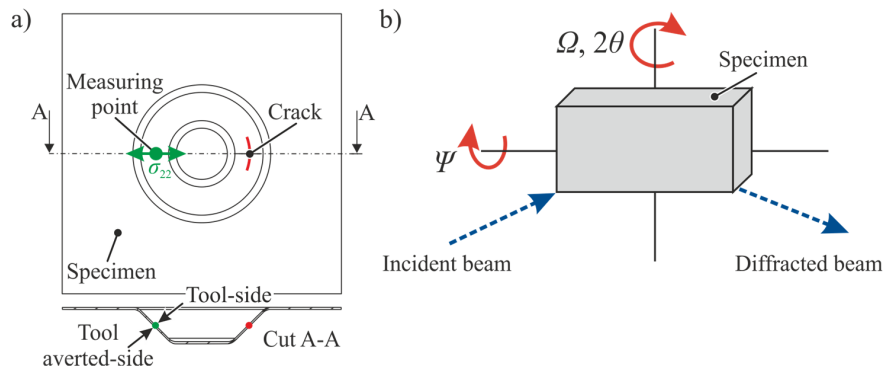


Figure 4. (a) Measuring point at the cone wall and (b) XRD measuring methodology.

2.4 Fatigue Test Setup

A fatigue test is performed to illustrate the influence of the manufacturing process on the fatigue strength of the formed component. The servo-hydraulic testing equipment MTS 810 for dynamic tensile and compression tests is used for the fatigue tests. During the testing procedure, the specimens are mounted at the edges and at the bottom of the truncated cone to the testing equipment, fixtures to apply the cyclic loading (see Figure 5a). A cyclic load $F_{ax} = 600$ N is applied to the specimen with a frequency $f = 10$ Hz (see Figure 5b). The fatigue test is finished when a visible crack occurs at the sidewall of the cone geometry. To evaluate the influence of the residual stresses on the fatigue strength of the component, reference tests are performed with stress-relieved truncated cone components. Specimens with step-down increments $\Delta z_{0.25} = 1.25$ mm, $\Delta z_{0.5} = 2.5$ mm and $\Delta z_{0.75} = 3.75$ mm are stress-relieved by heat treatment. The specimens are heat-treated for 2 min with 300 °C including 1 min holding time. Residual stress measurements after the heat treatment show that there are no significant residual stresses left ($\sigma_{22} = 1 \pm 9$ MPa in the measuring point) in the component the low temperature and short heat treatment period ensures that there is no effect on the microstructure of the material.

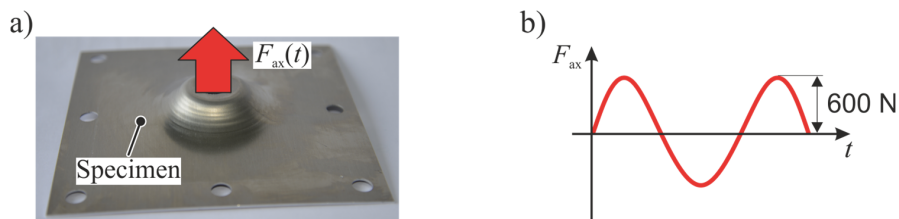


Figure 5. (a) Fatigue test set-up and (b) force amplitude.

3 Results and Discussion

3.1 Residual Stress State

The residual stresses are measured in the middle of the curved surface area of the truncated cone in radial direction σ_{22} . This stress direction is relevant for a crack initiated in circumferential direction due to the applied loading on the bottom of the truncated cone. On the tool-side tensile residual stresses are measured that decrease with decreasing with the number of step-down increments in radial direction (see Figure 6a). The moderate tensile residual stresses ($\sigma_{22} = 82 \pm 20$) for 12 step-down increments ($\Delta z/R_{tool} = 0.25$) are slightly decreased about 4% for half number of increments ($\Delta z/R_{tool} = 0.5$) but nearly vanish if four step-down increments

($\sigma_{22} = 3 \pm 10$) are used. The compression residual stresses on the tool-averted side are less widespread than the tensile residual stresses on the tool-side (see Figure 6b). This is due to the friction between the forming tool and the sheet whereby the residual stresses are more pronounced on the tool-side. The compression residual stresses on the tool-averted side are almost stationary with an increasing number of step-down increments and vary in a range of 30% for the investigated range. The numerical results evaluated in the same measuring point show a similar trend for both sides of the truncated cone geometry. The predictions of the residual stress amplitudes with an average deviation of 16% are in good accordance with the experimental results considering the measuring tolerances.

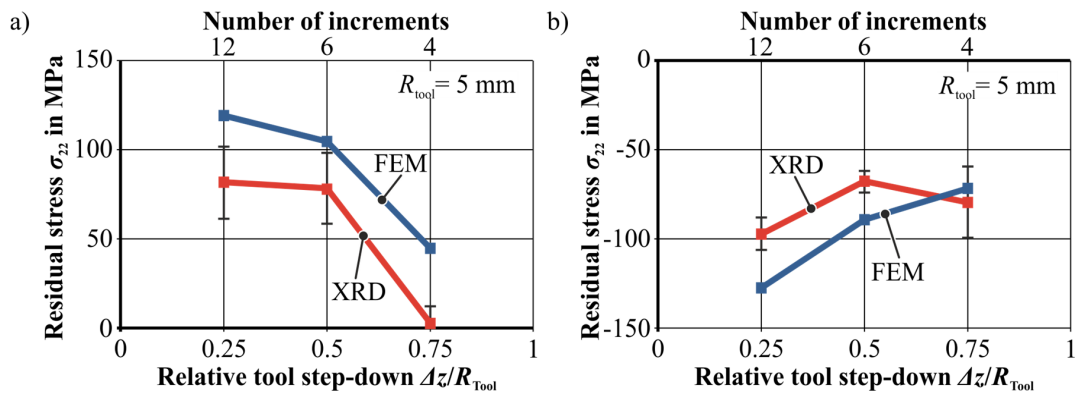


Figure 6. (a) Residual stresses (a) on the tool-side and (b) on the tool-averted side.

3.2 Sheet Thickness

The sheet thickness is evaluated in the measuring point at the sidewall of the truncated cone for three different relative tool step-down increments. The sheet thickness decreases monotonously with the total number of step-down increments used. Sheet thinning is typical for single point incremental forming due to the clamped sheet edges. The sheet thickness decreases about 22% from 840 ± 11 μm for four step-down increments to 690 ± 11 μm for 12 step-down increments (see Figure 7a). The numerically evaluated hardening of the material in the measuring point increases in an opposing trend due to the thinning. Consequently, the residual stress amplitudes rise with increasing strain hardening (Figure 7b), since the locked stresses due to unloading after plastic deformation are greater then.

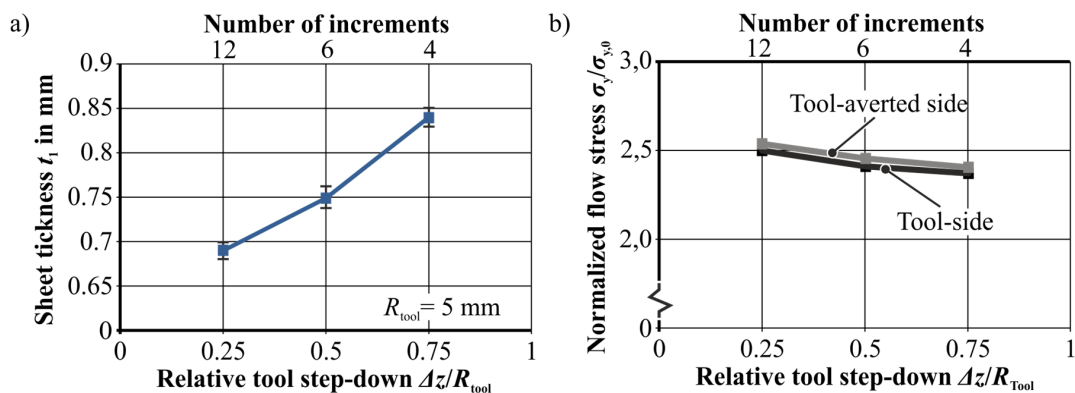


Figure 7. (a) Sheet thickness (experimental values) and (b) normalized material hardening (FEM) in the measuring point.

3.3 Fatigue Strength

Finally, the influence of the manufacturing-induced residual stresses on the fatigue strength of the truncated cones formed with three different parameter set is tested. The results of the cyclic loading tests as shown in Figure 8 illustrate that the fatigue strength is increasing with a decreasing number of step-down increments used. The fatigue strength can be improved by 174% within the range of process parameters investigated. From 188,000 cycles until crack initiation for $\Delta z/R_{\text{tool}} = 0.25$ the fatigue strength can be improved to 515,000 cycles until crack initiation for $\Delta z/R_{\text{tool}} = 0.75$ in absolute numbers. The fatigue strength of the stress-relieved specimens is increasing with a decreasing number of step-down increments as well. This means that the same fatigue strength can be reached without heat treatment for the case $\Delta z/R_{\text{tool}} = 0.75$.

Regarding the thinning of the cone wall, the wall thickness is increased with a decreasing number of step-down increments. Thus, the decreasing fatigue strength of the stress-relieved specimens is caused by the thinning of the cone wall. If the results for the cyclic loading tests of the untreated and stress-relieved specimens are compared, the influence of residual stresses can be quantified. Due to residual stresses, the fatigue strength of the component is decreased up to 42%. The increasing tensile residual stresses on the tool-side are responsible for the reduced fatigue strength of a component (see Figure 6).

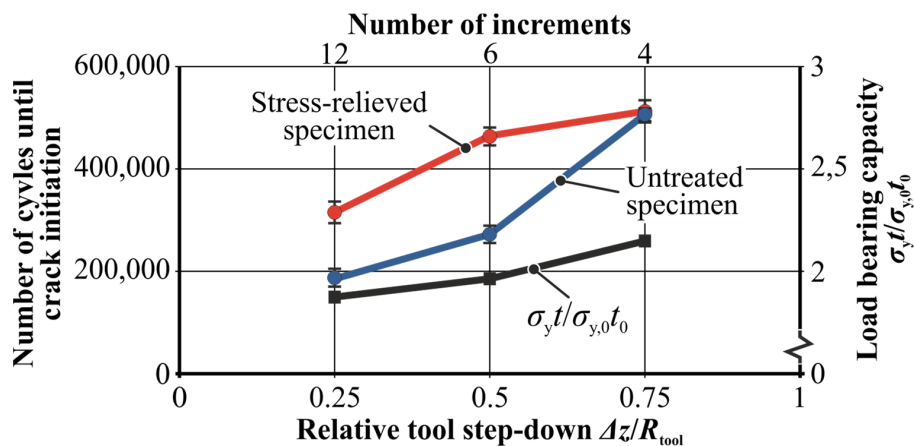


Figure 8. Cyclic loading test for increasing relative tool step-down.

4 Conclusion

It was shown that the fatigue strength of SPIF components, especially cyclic-loaded ones can be improved by adjusting the residual stresses through the choice of process parameters. Residual stresses were evaluated by XRD measurements and numerical simulations to show that tensile residual stresses on the tool-side can be reduced by increasing the relative tool step-down increment. Besides the thinning in combination with the hardening behavior, these tensile residual stresses on the tool-side are responsible for the reduced fatigue strength. By eliminating these tensile residual stresses within the SPIF process, an improved fatigue strength can be observed. Current investigations deal with the process enhancements on how to even induce compressive residual stresses on the tool-side to further increase the fatigue strength of SPIF components.

Acknowledgement

The authors would like to thank the German Research Foundation (DFG - Deutsche Forschungsgemeinschaft) for funding the research projects RE 688/76-1 and TE 508/67-1.

References

1. M. Brettel, M. Klein, N. Friederichsen, "The Relevance of Manufacturing Flexibility in the Context of Industrie 4.0," *Procedia CIRP*, 41 (2016), 105-110.
2. K. P. Jackson, J. M. Allwood, "The Mechanics of Incremental Sheet Forming," *Journal of Materials Processing Technology*, 209 (3) (2009), 1158-1174.
3. J. Tuomi, L. Lamminen, "Incremental Sheet Forming as a Method for Sheet Metal Component Prototyping and Manufacturing" (10 èmes Assises Européennes de Prototypage Rapide 2004), 1.
4. J. Jeswiet, "Rapid Proto-Typing with Incremental Single Point Forming" *Revue internationale de CFAO et d'informatique graphique*, 15 (2-4) (2000), 177-184.
5. C. Radu, E. Herghelegiu, C. Tampu, I. Cristea, "The Residual Stress State Generated by Single Point Incremental Forming of Aluminum Metal Sheets," *Applied Mechanics and Materials*, 371 (2013), 148-152.
6. F. Maaß, M. Dobecki, A. Poeche, M. Hahn, K. Brömmelhoff, W. Reimers, A. E. Tekkaya, "Forming Mechanisms-related Residual Stress Development in Single Point Incremental Forming," *AIP Conference Proceedings*, 1960 (1) (2018).
7. F. Maaß, S. Gies, S., M. Dobecki, K. Brömmelhoff, W. Reimers, A. E. Tekkaya, "Analysis of residual stress state in sheet metal parts processed by single point incremental forming.," *Production Engineering - Research and Development*, 13 (149) (2019), 149-156.
8. E. Macherauch E, P. Müller P, "Das $\sin^2\text{-}\Psi$ Verfahren von röntgenographischen Eigenspannungen," *Zeitschrift für angewandte Physik*, 13 (1961), 305-312.